Systems/Circuits

Multiple Sensory Inputs Are Extensively Integrated to Modulate Nociception in *C. elegans*

Philip J. Summers,[1]* Robert M. Layne,[1]* Amanda C. Ortega,[1] Gareth P. Harris,[2] Bruce A. Bamber,[1] and Richard W. Komuniecki[1]

[1]Department of Biological Sciences, University of Toledo, Toledo, Ohio 43606, and [2]Department of Organismic and Evolutionary Biology, Center for Brain Science, Harvard University, Cambridge, Massachusetts 02138

Sensory inputs are integrated extensively before decision making, with altered multisensory integration being associated with disorders such as autism. We demonstrate that the two *C. elegans* AIB interneurons function as a biphasic switch, integrating antagonistic, tonic, and acute inputs from three distinct pairs of sensory neurons to modulate nociception. Off food, animals reverse away from a noxious stimulus. In contrast, on food or serotonin, AIB signaling is inhibited and, although animals initiate an aversive response more rapidly, they continue forward after the initial backward locomotion is complete. That is, animals continue to move forward and feed even when presented with a noxious repellant, with AIB inhibition decreasing the repellant concentration evoking a maximal response. These studies demonstrate that the AIBs serve as an integrating hub, receiving inputs from different sensory neurons to modulate locomotory decision making differentially, and highlight the utility of this model to analyze the complexities of multisensory integration.

Key words: **behavior; *C. elegans*; electrophysiology; sensory integration**

Significance Statement

Dysfunctional sensory signaling and perception are associated with a number of disease states, including autism spectrum disorders, schizophrenia, and anxiety. We have used the *C. elegans* model to examine multisensory integration at the interneuron level to better understand the modulation of this complex, multicomponent process. *C. elegans* responds to a repulsive odorant by first backing up and then either continuing forward or turning and moving away from the odorant. This decision-making process is modulated extensively by the activity state of the two AIB interneurons, with the AIBs integrating an array of synergistic and antagonistic glutamatergic inputs, from sensory neurons responding directly to the odorant to others responding to a host of additional environmental variables to ultimately fine tune aversive behaviors.

Introduction

One of the primary goals of neuroscience is to understand how sensory inputs interact to define behavioral state and ultimately modulate perception and behavior. Indeed, an inability to effectively integrate and process sensory information has been associated with disease states including autism, schizophrenia, posttraumatic stress disorder, attention deficit hyperactivity disorder, and depression (Kantrowitz and Javitt, 2010; Ghanizadeh, 2011; Mueller-Pfeiffer et al., 2013). The mammalian brain integrates an array of intrinsic and extrinsic cues to drive behaviors, and recent work suggests that most neocortical decision making is multisensory (Haider et al., 2006). *C. elegans*, with 14 pairs of sensory neurons and complex, sensory-mediated locomotory behaviors, provides an excellent model with which to study context-dependent multisensory interactions. For example, nociception and aversive responses mediated by the two ASH sensory neurons can be initiated through two distinct circuits, each of which is modulated independently to direct locomotory decision making (Piggott et al., 2011). Sensory-evoked aversive responses can be initiated by activation of the two AVA backward command interneurons directly and/or signaling from the AIB/RIM circuit that antagonizes forward locomotion (Piggott et al., 2011). Indeed, ASH glutamatergic signaling is essential to initiate reversal in response to an array of noxious ligands (Mellem et al., 2002; Chao et al., 2004; Guo et al., 2009; Lindsay et al., 2011). The

Received Jan. 16, 2015; revised June 11, 2015; accepted June 14, 2015.

Author contributions: P.J.S., R.M.L., G.P.H., and R.W.K. designed research; P.J.S., R.M.L., and A.C.O. performed research; P.J.S., R.M.L., B.A.B., and R.W.K. analyzed data; P.J.S., R.M.L., and R.W.K. wrote the paper.

This work was supported by the National Institutes of Health (Grant AI072644 to R.W.K.), the Whitehall Foundation to (B.A.B.), and the Joan L. and Julius H. Jacobson Biomedical Professorship. We thank the *C. elegans* Genetics Center and the National Bioresources Center for strains; Cori Bargmann for inx-1::GCaMP3, odr-2 (2b)::glr-1::gfp, and inx-1::HisCl1; Sreekanth Chalasani for gcy-5::GCaMP3 and str-2::GCaMP3 in *unc-13* and *unc-31* backgrounds; and Shawn Xu for nmr-1::glr-1 rescue in *glr-1* background.

The authors declare no competing financial interests.

*P.J.S. and R.M.L. are co-first authors.

Correspondence should be addressed to Richard Komuniecki, Department of Biological Sciences, University of Toledo, 2801 W. Bancroft Street, Toledo, OH 43606-3390. E-mail: rkomuni@uoft02.utoledo.edu.

DOI:10.1523/JNEUROSCI.0225-15.2015

 0270-6474/15/3510331-12$15.00/0

ASH-mediated aversive circuit is modulated directly by an array of context-dependent cues, with signaling from a host of synaptic and extrasynaptic monoamine and neuropeptide receptors modulating locomotory decisions (Harris et al., 2010; Harris et al., 2011; Mills et al., 2012b; Hapiak et al., 2013). For example, the food or 5-HT-dependent modulation of ASH-mediated aversive responses to the repellant 1-octanol requires three distinct serotonin (5-HT) receptors, each operating at a different level in the aversive circuit. Similarly, 5-HT also modulates sensory integration in mammals; for example, 5-HT imposes context-dependent plasticity in the modulation of auditory processing (Hanson and Hurley, 2014).

In the present study, we have defined how inputs from three distinct pairs of sensory neurons are integrated by the two AIB interneurons to modulate locomotory behaviors. The sensory ASHs and AWCs both innervate the AIBs directly and respond antagonistically to 1-octanol, with AIB signaling modulated by both excitatory and inhibitory AIB glutamate receptors. Off food, AIB signaling is stimulated and most animals back up, execute an ω turn, and move away from the source of the repellant. In contrast, on food, 5-HT levels are elevated, AIB signaling is inhibited, and, although animals initiate an aversive response more rapidly, they back up less and continue forward toward the noxious stimulus after the initial backward locomotion (BL) is complete. That is, animals will continue to move toward food and feed even in the face of a noxious, potentially dangerous, odorant. Similarly, the salt-sensing ASER also extensively innervates the AIBs and, although ASER does not respond directly to 1-octanol, ASER activation alters aversive responses in a manner identical to the presence of food or 5-HT. Together, these results demonstrate that the AIBs serve as an integrating hub, receiving inputs from an array of sensory neurons to fine-tune locomotory decision making.

Materials and Methods

Behavioral assays. For all behavioral assays, hermaphrodite fourth-stage larvae were picked 24 h before testing. Nematode growth medium (NGM) plates were prepared the day of behavioral assays, with 5-HT, histamine, or *E. coli* strain OP50. Aversive responses to dilute (30%) 1-octanol, reversal frequency, and aversive responses were examined as described previously (Chao et al., 2004; Harris et al., 2009; Harris et al., 2010; Harris et al., 2011; Mills et al., 2012b). Briefly, we examined forward moving animals and recorded the following: (1) the time taken to initiate BL after presentation of 30% 1-octanol, (2) the number of body bends during BL, and (3) the direction the animals turned after BL. Isoamyl alcohol (IAA) and NaCl were used to manipulate AWC and ASE signaling, respectively. To inhibit AWC activity, IAA (40% v/v) was mixed in EtOH with varying concentrations of 1-octanol and 1-octanol avoidance was assayed as described above. To stimulate ASEL activity with a salt up-step, animals were incubated on NGM plates and transferred to NGM (50 mM NaCl) plates +10 mM NaCl for 10 min and 1-octanol avoidance assayed after 2 min, as described above. To stimulate ASER activity with a salt down-step, animals were transferred to NGM plates +10 mM NaCl for 10 min and then transferred to NGM plates and 1-octanol avoidance was assayed after 2 min, as described above (Suzuki et al., 2008; Oda et al., 2011). The rate of spontaneous reversal was assayed on and off food, as described previously (Gray et al., 2005). Spontaneous reversals are recorded as a break in forward locomotion followed by BL for one or more body bends. Each experiment was performed on three separate occasions, examining 15–20 individuals on each occasion. Data are presented as mean ± SEM and were analyzed using Student's *t* test with Welch's correction.

Molecular biology and transgenesis. For rescue/overexpression, cDNA or genomic regions corresponding to the entire coding sequences were amplified by PCR and expressed under cell-selective promoters. Selective expression was achieved using the *inx-1* (0.3 kb; AIB), *npr-9* (1.8 kb; AIB), *sro-1* (2.0 kb; ADLs), *sra-6* (3.3 kb; ASHs, ASIs, PVQs, SPDs/Ms), *flp-6* (2.0 kb; ASEs, AFDs, ASGs, PVT, I1), *gcy-5* (3.2 kb; ASER), *gcy-6* (0.5 kb; ASEL), *str-2* (3.7 kb, AWC), and *nlp-1* (2.5 kb; AWCs, ASIs, BDUs, HSN, PHBs, four head neurons) promoters, respectively. Experiments using *inx-1* were confirmed with a second AIB-selective promoter, *npr-9*, and similar results were observed. Promoter expression was confirmed by GFP expression and confocal microscopy. Neuron-selective rescue constructs were generated via overlap PCR fusion as described previously (Hobert, 2002). Neuron-selective RNAi's were generated as described previously (Esposito et al., 2007). PCR products were pooled from at least three separate reactions and injected with a selectable marker (*CC::rfp* or *myo-3::gfp*) with salmon sperm carrier DNA into the gonads of hermaphrodite *C. elegans* wild-type or-null mutants by standard techniques (Kramer et al., 1990; Mello et al., 1991).

Glutamate application. To characterize glutamate responses in AIBs, hermaphrodite animals were glued to Sylgard (Dow Corning)-coated coverslips using WormGlu cyanoacrylate glue (GluStitch) while immersed in electrophysiology external solution containing the following (in mM): NaCl 150, KCl 5, $CaCl_2$ 5, $MgCl_2$ 1, glucose 10, and HEPES 15, pH 7.30, 330 mOsm. The coverslip was then placed in a laminar flow chamber (RC26G, Warner Instruments) mounted on an Axioskop 2 FS Plus upright compound microscope (40× Achroplan water-immersion objective, GFP filter set #38) and perfused with external solution.

For intracellular calcium (Ca^{2+}i) imaging, animals were dissected longitudinally and external solution containing 500 μM glutamate was applied using a multibarrel fast perfusion system (Warner Instruments SF77B, barrel width 300 μm) that was controlled by pCLAMP10 acquisition software (Molecular Devices).

For electrophysiology, animals either had an AIB cell body exposed with a small incision in the cuticle using standard protocols (Goodman et al., 1998; Piggott et al., 2011) or were more fully dissected with a second incision longitudinally on the contralateral side to expose the entirety of the AIB interneurons to the drug-containing solution. Glutamate was applied as described above. The microscope was fitted with an Orca ER CCD camera and programmable shutter (Uniblitz; Vincent Associates) was used to perform GCaMP3 recordings and patch-clamp electrophysiology. MetaVue 7.6.5 (MDS ANALytical Technologies) was used to capture fluorescence images. Patch-clamp recordings were performed as described previously (Goodman et al., 1998) using an Axon Axopatch 2B amplifier and Axon Digidata 1440 digitizer (Molecular Devices). Fluorescent images were analyzed using Jmalyze software (Rex Kerr). Samples were acquired at ~20 Hz (50 ms exposure time) with 4× binning. Voltage-clamp recordings were filtered using a Butterworth (8-pole) low-pass filter with a −3 dB cutoff of 100 Hz.

Odorant application. To image the effects of 1-octanol, hermaphrodite animals expressing *sra-6*::GCaMP3 in wild-type animals and *str-2*::GCaMP3 in wild-type, *unc-13*, and *unc-31* backgrounds were glued to coverslips immersed in NaCl 50 mM, KPO_4 5 mM, $MgSO_4$ 1 mM, and $CaCl_2$ 1 mM. The coverslip was then placed in a laminar flow chamber under the microscope perfused with a saline, followed by saline containing a saturating 1-octanol concentration (2.3 μM) applied using a multibarrel fast perfusion system. The same setup used to capture the glutamate-evoked changes in AIB calcium was used to capture 1-octanol-evoked changes in neuronal calcium. Samples were acquired at ~10 Hz (100 ms exposure time) with 4 × binning.

Results

ASH-mediated aversive responses to dilute 1-octanol can be divided into three phases: (1) the time taken to initiate BL, (2) the length of the BL, and (3) the post-BL decision to either move away from the noxious odorant or continue forward after the initial BL is complete (Fig. 1*A*) (Harris et al., 2011). The time taken to initiate the aversive response appears to be largely bimodal, depending on nutritional status (Fig. 1*B*) (Harris et al., 2011). For example, when a hair dipped in dilute (30%) 1-octanol is placed in front of a wild-type animal moving forward, BL was initiated in ~10 s off food and in ~5 s on food ($t = 11.1$, df = 92,

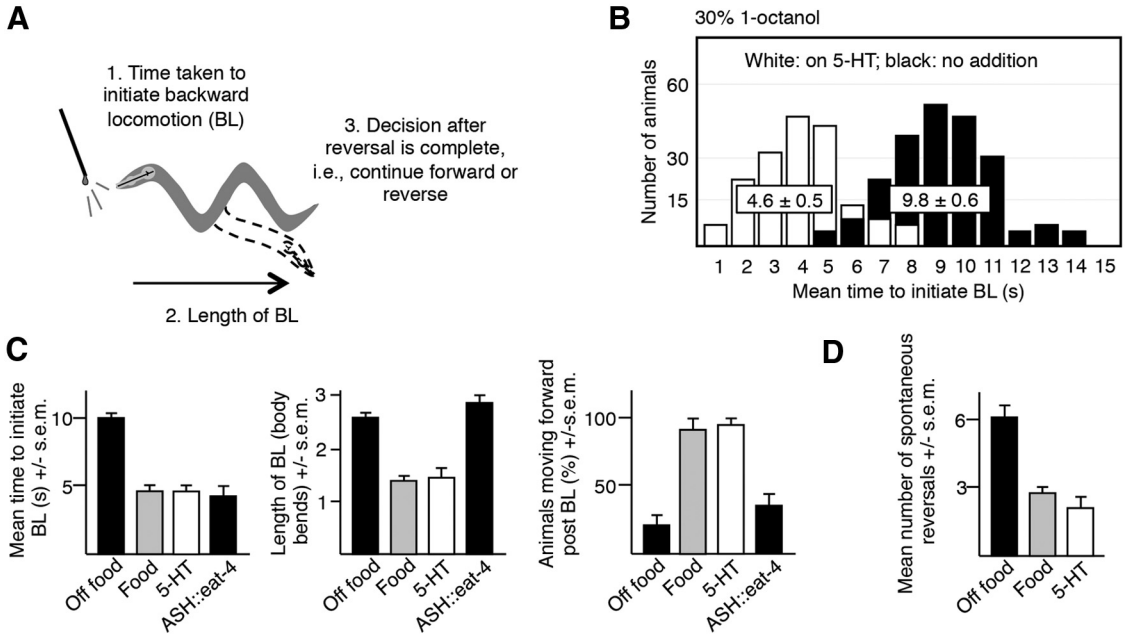

Figure 1. ASH-mediated aversive responses to dilute 1-octanol are biphasic with individual components modulated independently by nutritional status. ***A***, Diagram of the aversive response to dilute 1-octanol, including responses to the initial aversive stimulus and postinitiation responses after 1-octanol-evoked BL is initiated. ***B–D***, Aversive responses to dilute 1-octanol with and without food plus 4 mM 5-HT and spontaneous reversals were examined in wild-type and transgenic animals. The *eat-4* cDNA was expressed under the *sra-6* promoter in a wild-type background. Data represent mean ± SEM with 15–20 animals being tested in 3 independent experiments and were analyzed by two-tailed Student's *t* test with Welch's correction. *$p < 0.001$, significantly different from wild-type animals under identical conditions.

$p < 0.001$) or after preincubation in exogenous 5-HT ($t = 11.6$, df = 123, $p < 0.001$;Fig. 1*B*). In fact, most manipulations of the ASH-mediated locomotory circuit result in animals responding in either ~5 or 10 s, suggesting that some portion of the circuit may be functioning as a bimodal switch (Chao et al., 2004; Harris et al., 2009; Harris et al., 2010). Each phase of the process appears to be modulated independently. For example, off food, most animals backed up and then moved away from the noxious stimulus. In contrast, on food or exogenous 5-HT, animals initiated the aversive response more rapidly (~5 vs 10 s) but, paradoxically, backed up less (food: $t = 9.3$, df = 101, $p < 0.001$; 5-HT: $t = 5.7$, df = 115, $p < 0.001$) and then proceeded forward toward the source of the noxious stimulus (food: $t = 10$, df = 74, $p < 0.001$; 5-HT: $t = 8.6$, df = 106, $p < 0.001$); that is, animals were willing to put up with a bad smell if they were feeding, but not if they were hungry (Harris et al., 2011; Fig. 1*B*,*C*). Interestingly, ASH *eat-4* overexpression, predicted to increase glutamatergic signaling from the ASHs, stimulated the initiation of the aversive response from ~10 to ~5 s ($t = 8.6$, df = 71, $p < 0.001$), but had no effect on subsequent locomotory behavior, suggesting that the length of the BL and the ultimate decision to continue to move forward or backward were modulated independently (Fig. 1*C*). Interestingly, although 5-HT stimulated the initiation of the aversive response, 5-HT decreased the rate of spontaneous reversal ($t = 10$, df = 38, $p < 0.001$), also suggesting that aspects of sensory-evoked and spontaneous reversal also might be modulated independently (Fig. 1*D*).

AIB interneurons influence both the initiation of the aversive response and the decision to move forward or reverse after sensory-evoked BL is complete

To better understand the role of the AIBs in spontaneous and sensory-evoked reversal, the AIBs were ablated by the AIB expression of a cell death protein encoded by *egl-1* (Conradt and Horvitz, 1998). AIB ablation dramatically decreased the time taken to initiate an aversive response off food from ~10 to ~5 s ($t = 10.1$, df = 77, $p < 0.001$), but induced animals to back up less ($t = 8.2$, df = 86, $p < 0.001$) and move forward after BL was complete ($t = 9$, df = 53, $p < 0.001$) as if they were on food (Fig. 2*A*). In contrast, AIB ablation decreased the frequency of spontaneous reversal immediately off food ($t = 10.2$, df = 42, $p < 0.001$), as noted by others, but again induced the animals to move forward after BL was complete ($t = 4.2$, df = 39, $p < 0.001$) as if they were on food. That is, the inhibition of AIB signaling induced forward movement whether the initial BL was spontaneous or sensory evoked (Fig. 2*B*; Gray et al., 2005). These observations suggest that the AIBs might exist in two different activity states, one favoring the more rapid initiation of a 1-octanol-dependent aversive response, followed by forward movement toward the noxious odorant, and one favoring a slower initiation of the aversive response, followed by a reversal and movement away from the noxious source.

To examine this hypothesis, AIB signaling was selectively increased or decreased by overexpression or knock-down of key signaling molecules. For example, AIB signaling was decreased by the AIB expression of the following: (1) a synaptobrevin-specific protease, tetanus toxin (TeTx), which is predicted to decrease AIB neurotransmitter release (Busch et al., 2012); (2) eat-4 RNAi, which is predicted to decrease the expression of an AIB vesicular glutamate transporter and glutamate release; and (3) MOD-1, a 5-HT gated Cl^- channel that is predicted to hyperpolarize the AIBs. In contrast, AIB signaling was selectively increased by the AIB expression of GLR-1, an AMPA-like glutamate receptor subunit that is predicted to depolarize the AIBs and mod-1 RNAi. Both GLR-1 and MOD-1 have been identified previously in the AIBs, with GLR-1 essential for AWC-mediated food chemotaxis and MOD-1 required for the 5-HT stimulation of aversive responses (Chalasani et al., 2007; Harris et al., 2009). The AIB ex-

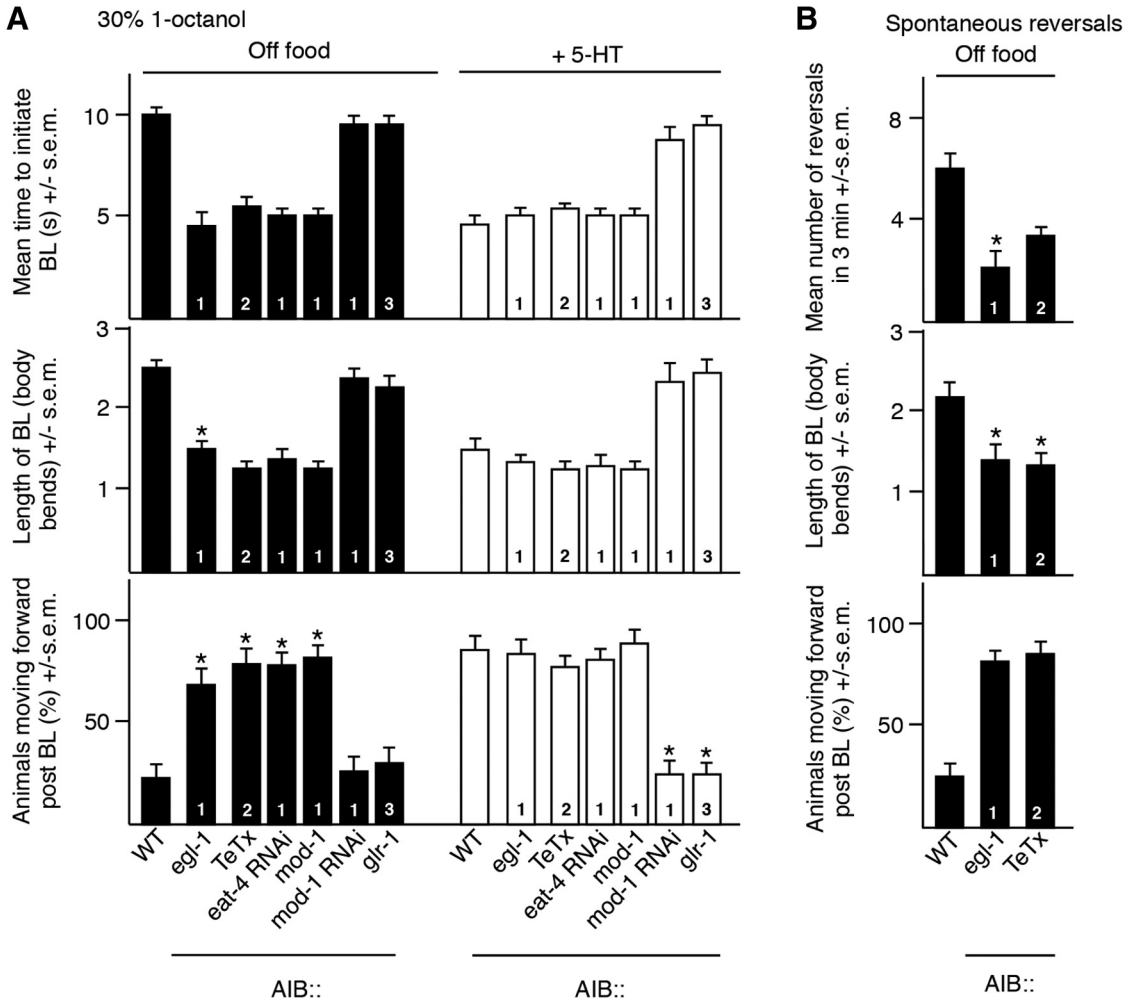

Figure 2. AIB signaling modulates both spontaneous and sensory-evoked reversal behavior differentially. ***A***, ***B***, Aversive responses to dilute 1-octanol without and with 4 mM 5-HT (black and white bars, respectively) and spontaneous reversals were examined in wild-type and transgenic animals. *egl-1*, TeTx, *mod-1*, and *glr-1* cDNAs were expressed in the AIBs under the *npr-9* or *inx-1* promoters in wild-type backgrounds. *npr-9*, *inx-1*, and *odr-2(2b)* promoters are labeled as 1, 2, and 3, respectively. *eat-4*- and *mod-1*-selective RNAi was performed using the *npr-9* promoter. Data represent mean ± SEM with 15–20 animals being tested in 3 independent experiments and were analyzed by two-tailed Student's *t* test with Welch's correction. *$p < 0.001$, significantly different from wild-type animals under identical conditions.

pression of TeTx, eat-4 RNAi, or MOD-1 in wild-type animals, predicted to decrease AIB signaling, decreased the time taken to initiate 1-octanol-dependent BL (TeTx: $t = 11.3$, df = 111, $p < 0.001$; eat-4 RNAi: $t = 8.5$, df = 58, $p < 0.001$; MOD-1: $t = 11.8$, df = 83, $p < 0.001$) and induced these transgenic animals to back up less (TeTx: $t = 3.7$, df = 91, $p < 0.001$; eat-4 RNAi: $t = 4.5$, df = 54, $p < 0.001$; MOD-1: $t = 3.4$, df = 62, $p < 0.001$) and move forward after BL was complete (TeTx: $t = 7.4$, df = 85, $p < 0.001$; eat-4 RNAi: $t = 6.6$, df = 44, $p < 0.001$; MOD-1: $t = 6.9$, df = 56, $p < 0.001$; Fig. 2*A*). Similarly, decreasing AIB signaling also decreased the rate of spontaneous reversal off food (EGL-1: $t = 10.2$, df = 42, $p < 0.001$; TeTx: $t = 5.4$, df = 52, $p < 0.001$; Fig. 2*B*). In contrast, the expression of AIB GLR-1 or mod-1 RNAi in wild-type animals, predicted to increase AIB signaling, had no effect on locomotory behavior off food, but abolished the effect of 5-HT on all three phases of the 1-octanol-dependent aversive response by increasing the time to initiate (GLR-1: $t = 7.5$, df = 27, $p < 0.001$; mod-1 RNAi: $t = 5.9$, df = 23, $p < 0.001$), increasing the length of BL (GLR-1: $t = 5$, df = 58, $p < 0.001$; mod-1 RNAi: $t = 6.2$, df = 58, $p < 0.001$), and decreasing the number of animals moving forward after BL is complete (GLR-1: $t = 4.3$, df = 33, $p < 0.001$; mod-1 RNAi: $t = 4.4$, df = 36, $p < 0.001$; Fig. 2*A*).

Because the interpretation of these genetic manipulations is potentially complicated by developmental compensation, the AIBs were acutely hyperpolarized and inactivated by expression of a histamine-gated Cl^- channel, HisCl1, followed by incubation in histamine, as described previously (Pokala et al., 2014). As predicted, the AIB expression of AIB HisCl1 alone had no effect on aversive responses (Fig. 3*A*). In contrast, the histamine activation of AIB HisCl1 decreased the time taken to initiate BL ($t = 8.4$, df = 82, $p < 0.001$), decreased the length of the BL ($t = 8$, df = 99, $p < 0.001$), and induced animals to move forward after BL was complete ($t = 9.7$, df = 77, $p < 0.001$; Fig. 3*A*). In addition, AIB HisCl1 activation also decreased the rate of spontaneous reversal ($t = 10.5$, df = 48, $p < 0.001$; Fig. 3*B*). To confirm the central role of the AIBs in differentially modulating motor outputs, we titrated the histamine concentration used for AIB hyperpolarization (Fig. 3*C*). Using this approach, we could separate the effects of AIB hyperpolarization on initiation and postinitiation responses and demonstrate that individual aspects of the aversive response were exquisitely sensitive to the activation state of the

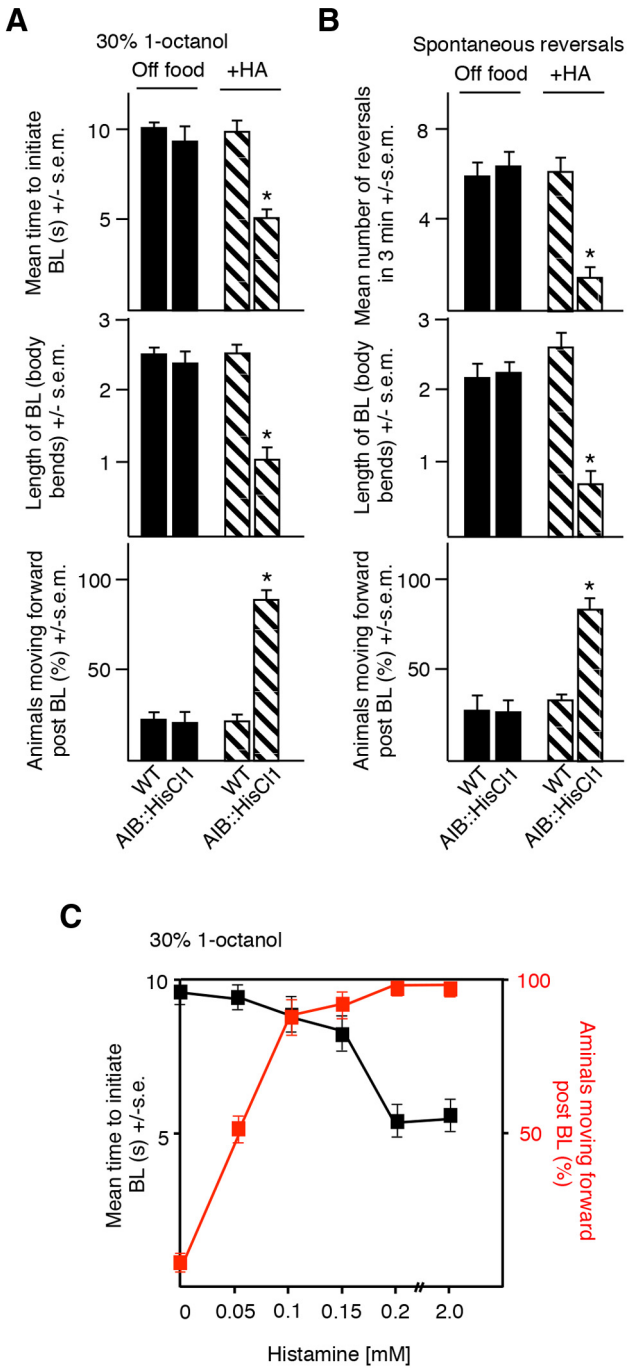

Figure 3. Acute AIB hyperpolarization by a heterologously expressed HisCl1 histamine-gated Cl^- channel modulates both spontaneous and sensory-evoked behavior. ***A***, ***B***, Aversive responses to dilute 1-octanol without and with 4 mM HA (black and patterned bars, respectively) and spontaneous reversals were examined in wild-type and transgenic animals. HisCl1 cDNA was expressed in the AIBs under the *inx-1* promoter in wild-type background. ***C***, Aversive responses to dilute octanol in animals expressing HisCl1 selectively in the AIBs to varying concentrations of HA. Data represent mean ± SEM with 15–20 animals being tested in 3 independent experiments and were analyzed by two-tailed Student's *t* test with Welch's correction. *$p <$ 0.001, significantly different from wild-type animals under identical conditions.

AIBs. For example, histamine concentrations >0.2 mM decreased the time taken to initiate BL and induced animals to move forward after BL was complete. In contrast, 0.15 mM histamine had no effect on the time taken to initiate an aversive response (8.8 ± 0.6 vs 9.2 ± 0.8 s for wild-type animals), but still induced forward locomotion (88% vs 0% for wild-type animals; Fig. 3*C*). Together, these data support our hypothesis that the inhibition of AIB signaling decreases the time taken to initiate 1-octanol-dependent BL, but also induces animals to back up less and move forward after BL is complete, just as it inhibits spontaneous reversal, but also suggest that individual components of the response can be modulated independently, depending on the activity state of the AIBs.

AWC sensory neurons also respond 1-octanol and modulate aversive behavior

The polymodal AWCs also innervate the AIBs and, surprisingly, also appeared to respond directly to 1-octanol, with 1-octanol increasing ASH and decreasing AWC somal Ca^{2+} transients (Chalasani et al., 2007; Mills et al., 2012a). The two AWC sensory neurons can also function as interneurons in the salt circuit (Leinwand and Chalasani, 2013). Therefore, to examine this possibility, we assayed AWC calcium response in *unc-13*- and *unc-31*-null animals predicted to be deficient in synaptic vesicle and dense core vesicle release, respectively (Kohn et al., 2000; Speese et al., 2007). Octanol-dependent decreases in AWC calcium were observed in both mutant backgrounds, but were significantly decreased in *unc-13*-null animals and increased in *unc-31*-null animals, highlighting the potentially extensive, context-dependent, modulation of AWC signaling observed previously (Leinwand and Chalasani, 2013). Importantly, although ASH eat-4 RNAi was previously demonstrated to abolish ASH glutamatergic signaling and aversive responses to dilute 1-octanol, it had no effect on 1-octanol-dependent AWC calcium responses (Harris et al., 2010). The AWCs are "off" neurons in that ligand addition lowers Ca^{2+}i so that the addition of 1-octanol would be predicted to decrease AWC signaling (Chalasani et al., 2007). AWC signaling inhibited the initiation of aversive responses to 1-octanol, because AWC-selective eat-4 RNAi knock-down or the addition of low concentrations of IAA predicted to decrease AWC signaling stimulated the initiation of aversive responses from ~10 to ~5 s (eat-4 RNAi: $t = 4.2$, df = 29, $p < 0.001$; Chalasani et al., 2007; Mills et al., 2012b). In addition, AWC eat-4 RNAi or IAA shortened the BL (eat-4 RNAi: $t = 5.3$, df = 41; IAA: $t = 4.4$, df = 45, $p < 0.001$) and dramatically increased the percentage of animals moving forward after BL was complete (eat-4 RNAi: $t = 8.6$, df = 34, $p < 0.001$; IAA: $t = 7.7$, df = 40, $p < 0.001$); that is, the animals behaved as if they were on food (Fig. 4*C*). Importantly, IAA alone did not initiate an aversive response (Mills et al., 2012b). Interestingly, AWC eat-4 overexpression abolished the 5-HT, but not the food, stimulation of aversive responses by decreasing the time to initiate BL ($t = 7.8$, df = 25, $p < 0.001$), increasing the length of BL ($t = 4.9$, df = 42, $p < 0.001$) and decreasing the percentage of animals moving forward after BL is complete ($t = 5$, df = 35, $p < 0.001$). Presumably food, but not 5-HT, suppressed AWC signaling (Chalasani et al., 2007). Consistent with this hypothesis, food also stimulated aversive responses in *tph-1*-null animals that lack tryptophan hydroxylase, a key enzyme in 5-HT biosynthesis, suggesting that this "food stimulation" in *tph-1*-null animals most probably resulted from a suppression of AWC activity (Chao et al., 2004). Indeed, as predicted, IAA also stimulated aversive responses in *tph-1*-null animals off food (Fig. 4*B*). Together, these data suggest that the ASHs are required for aversive responses to dilute 1-octanol, but that tonic signaling from the AWCs is suppressed by 1-octanol.

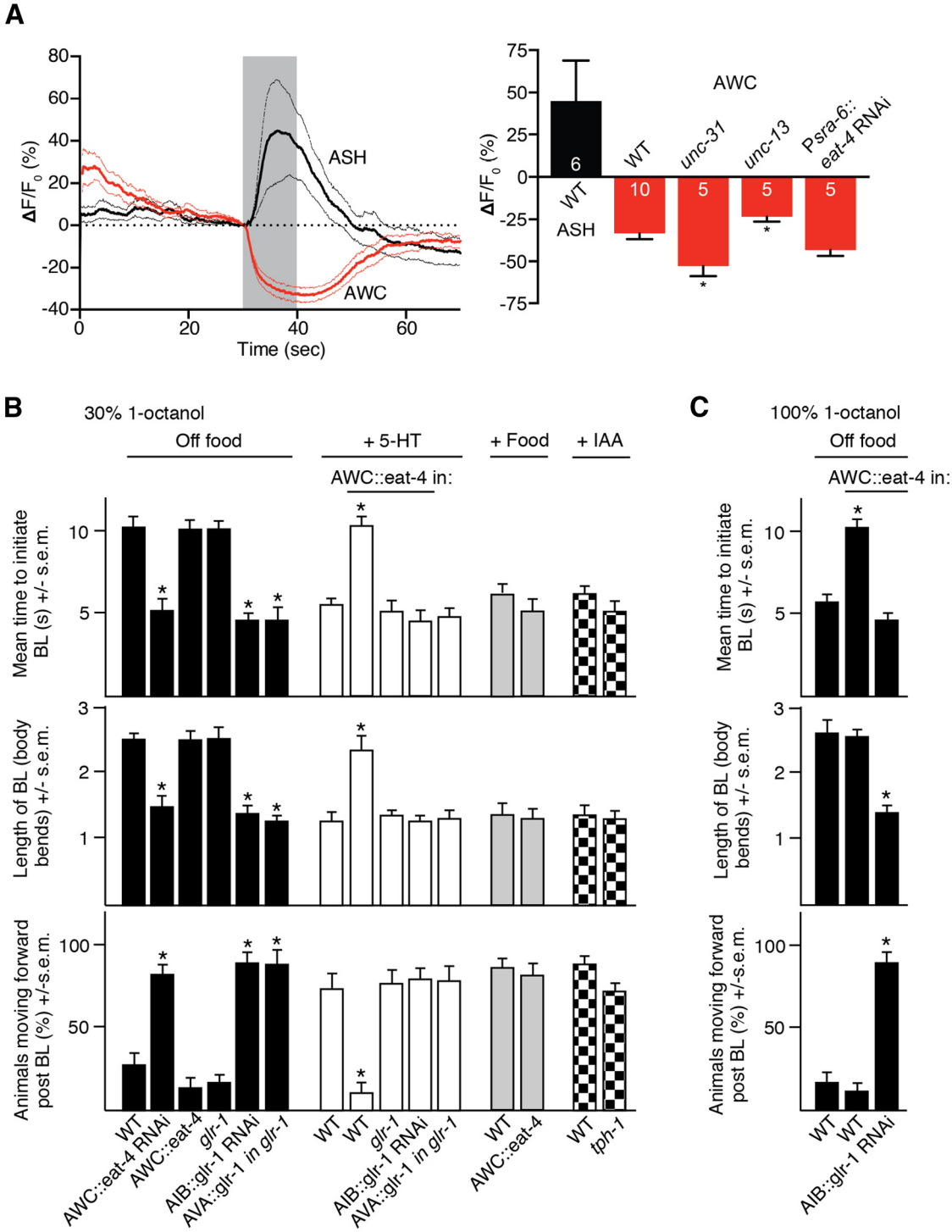

Figure 4. The AWC sensory neurons are inhibited by 1-octanol and AWC glutamatergic signaling to the AIBs abolishes 5-HT-stimulated aversive responses. ***A***, Trace average of octanol-evoked Ca^{2+}i transients in ASHs and AWCs of wild-type animals and maximum octanol-evoked Ca^{2+}i changes in ASHs of wild-type animals and AWCs of wild-type, *unc-13*, *unc-31*, and P*sra-6::eat-4* RNAi animals. Data are presented as mean ± SEM. Numbers within bars indicate *n*. ***B***, ***C***, Aversive responses to dilute (30%) and 100% 1-octanol without and with food, 4 mM 5-HT and IAA (black, white, gray and checkred bars, respectively) were examined in wild-type,-null and transgenic animals. *eat-4* was expressed in the AWCs using the *nlp-1* promoter. glr-1 RNAi and glr-1 cDNA was expressed in the AIBs and AVA using the *npr-9* and *nmr-1* promoters, respectively. Data represent mean ± SEM with 15–20 animals being tested in 3 independent experiments and were analyzed by two-tailed Student's *t* test with Welch's correction. *$p < 0.001$, significantly different from wild-type animals under identical conditions.

Glutamatergic signaling from the AWC sensory neurons activates the AIBs and abolishes the 5-HT sensitization of aversive responses

As noted above, the AWCs appear to respond to 1-octanol directly. Previous work has demonstrated the glutamatergic signaling from the AWCs activated an AIB AMPA-like glutamate receptor, GLR-1, so we examined the role of AIB GLR-1 in responses to dilute 1-octanol (Chalasani et al., 2007). As predicted, AIB RNAi knock-down of *glr-1* mimicked the AWC RNAi knock-down of *eat-4* and stimulated the initiation aversive re-

sponses off food from ~10 to ~5 s ($t = 11.1$, df = 106, $p < 0.001$), shortened the BL ($t = 6.6$, df = 99, $p < 0.001$), and induced forward movement after BL ($t = 8.8$, df = 70, $p < 0.001$), supporting previous observations that AWC signaling activated the AIBs through AIB GLR-1 (Chalasani et al., 2007). In contrast, although AIB::glr-1 RNAi animals initiated BL in ~5 s off food, *glr-1*-null animals initiated BL in ~10 s, arguing for a more complex role for GLR-1 signaling in ASH-mediated aversive responses (Fig. 4*C*). Indeed, synapses between the ASHs and the AVA backward command interneurons are also glutamatergic and mediated, at least in part, by GLR-1. As predicted, *glr-1* expression specifically in the AVAs of *glr-1*-null animals decreased the time taken to initiate 1-octanol-dependent BL from 10 to 5 s compared with wild-type ($t = 11.1$, df = 114, $p < 0.001$) or *glr-1*-null animals ($t = 8.1$, df = 47, $p < 0.001$; Fig. 4*C*).

In addition to 5-HT, increasing the 1-octanol concentration from 30% to 100% also decreases the time taken to initiate 1-octanol-dependent BL off food from ~10 to ~5 s (Wragg et al., 2007; Harris et al., 2009; Harris et al., 2010; Harris et al., 2011; Mills et al., 2012b; Hapiak et al., 2013). Therefore, we predicted that animals overexpressing *eat-4* in the AWCs, predicted to increase AIB signaling, would also initiate aversive responses to 100% octanol more slowly than wild-type animals. Indeed, this was the case, with AWC::eat-4 overexpressors initiating BL off food in ~9 s in response to 100% 1-octanol ($t = 6.6$, df = 92, $p < 0.001$) and ~80% still reversing after BL was complete ($t = 0.3$, df = 86, $p = 0.7$; Fig. 4*D*). As predicted, AIB::glr-1 RNAi abolishes the slowed initiation observed after AWC::eat-4 overexpression ($t = 0.8$, df = 47, $p = 0.4$) and also causes most animals to move forward after BL is complete ($t = 8.3$, df = 42, $p < 0.001$), in contrast to wild-type animals or animals overexpressing AWC::eat-4 (Fig. 4*C*). Together, these data suggest that 1-octanol stimulates ASH GLR-1-mediated signaling and, conversely, inhibits AWC EAT-4 signaling into the AIBs, with AIB GLR-1 signaling antagonizing the 5-HT/MOD-1-dependent hyperpolarization of the AIBs essential for the 5-HT stimulation of aversive responses.

Glutamatergic signaling from the salt-sensing ASE sensory neurons inhibits the AIBs and increases aversive responses

The ASE sensory neurons also extensively innervate the AIBs and glutamatergic signaling from ASER modulates aversive responses to 1-octanol, although, in contrast to the ASHs and AWCs, the ASEs do not appear to respond to 1-octanol directly (White et al., 1986; Hapiak et al., 2013). For example, ASER *eat-4* overexpression decreases the time taken to initiate a 1-octanol-dependent aversive response ($t = 12.4$, df = 79, $p < 0.001$) and induces forward movement after BL ($t = 6.6$, df = 44, $p < 0.001$), suggesting that ASER glutamatergic signaling inhibits the AIBs (Hapiak et al., 2013). In contrast, ASER eat-4 RNAi knock-down abolishes 5-HT stimulation ($t = 6.6$, df = 52, $p < 0.001$; Fig. 5*A*). *C. elegans* contains a number of glutamate-gated Cl^- channel subunits, some of which (AVR-14, AVR-15) have been characterized previously by heterologous expression and genetic analysis (Arena et al., 1992; Dent et al., 2000; Cook et al., 2006). The more rapid aversive responses observed in animals overexpressing ASER::eat-4 were abolished in *avr-14lf* animals ($t = 4.1$, df = 34, $p < 0.001$), suggesting that the glutamate-gated Cl^- channel subunit AVR-14 was involved in ASER glutamatergic signaling (Fig. 5*A*). As predicted, the AIB RNAi knock-down of *avr-14* abolished the more rapid initiation of aversive responses ($t = 5.7$, df = 30, $p < 0.001$) observed in animals overexpressing ASER::eat-4 and also mimicked ASER eat-4 RNAi knock-down abolishing 5-HT stimulation (Fig. 5*A*). Conversely, wild-type animals overexpressing *avr-14* in the AIBs initiated aversive responses more rapidly than wild-type animals off food ($t = 10.4$, df = 66, $p < 0.001$) and continued forward after BL ($t = 4.1$, df = 31, $p < 0.001$; Fig. 5*A*).

ASE Ca^{2+}i responses to salt are asymmetric, with ASER responding to salt down-steps and ASEL salt up-steps. The more rapid initiation of aversive responses was only observed in animals overexpressing *eat-4* in ASER, suggesting that a salt down-step should mimic 5-HT and stimulate the initiation of an aversive response (Hapiak et al., 2013). Indeed, this was the case, with animals exposed to a salt down-step immediately increasing aversive responses to dilute 1-octanol from ~10 to ~5 s off food ($t = 13.9$, df = 96, $p < 0.001$) and continuing forward after BL was complete ($t = 7.4$, df = 48, $p < 0.001$), as observed for ASER::eat-4 overexpression (Fig. 5*B*). As predicted, although a salt down-step stimulated the initiation of the aversive response in wild-type animals, it had no effect on aversive responses in animals with an *avr-14lf* allele or expressing AIB::avr-14 RNAi (Fig. 5*B*). Overall, these data suggest that glutamatergic signaling from the AWCs and ASER function antagonistically to modify signaling from the AIBs through GLR-1 and AVR-14, respectively, and differentially modulate ASH-mediated aversive responses.

AIBs exhibit both excitatory GLR-1- and inhibitory AVR-14-dependent glutamate-gated currents

As noted above, the AIBs appear to express both the excitatory and inhibitory glutamate receptors GLR-1 and AVR-14, respectively. Therefore, this observation was examined directly using both electrophysiology and Ca^{2+}i imaging. Glutamate-dependent currents were recorded in the AIBs after AIB cell bodies were exposed by making a small incision in the cuticle. In wild-type animals, glutamate elicited a Cl^- current that was absent in *avr-14* animals ($t = 8$, df = 8, $p < 0.001$; Fig. 6*B*,*C*,*G*). The reversal potential of this current was −30 mV (Fig. 6*G*), consistent with a Cl^- conductance under the ionic conditions we used (Francis and Maricq, 2006). Surprisingly, glutamate did not evoke a cationic current in the AIBs of wild-type or *avr-14* animals (Fig. 6*B*,*C*). Therefore, assuming that glutamate access to GLR-1 receptors on the AIB processes might be compromised in these partially dissected preparations (Fig. 6*A*,*H*), glutamate-evoked currents in the AIBs were reexamined using animals that had an AIB cell body fully exposed after more extensive dissection (Fig. 6*D*,*H*; see Materials and Methods). Under these conditions, glutamate again evoked a robust Cl^- current in wild-type animals but, in contrast to the partially dissected preparations, also evoked a small current in *avr-14* animals (Fig. 6*E*–*G*). This current reversed at +15 mV (Fig. 6*G*), consistent with a cationic GLR-1-mediated current. As predicted, this response was absent in *avr-14*;*glr-1* animals ($t = 4.5$, df = 2, $p < 0.05$; Fig. 6*E*,*F*). These data suggest that AVR-14 is present on both AIB cell bodies and neurites, because AVR-14-mediated currents are observed when only the cell body is excised, and that GLR-1 is only present on distal portions of the neurite, because GLR-1-mediated currents are only observed when the animal is fully dissected open and the entirety of the AIB interneurons are exposed to the glutamate-containing solution (see Fig. 6*H*). To confirm these observations, we imaged glutamate-evoked changes of AIB Ca^{2+}i using the fully dissected preparation and glutamate elicited a reduction of AIB Ca^{2+}i in wild-type animals, consistent with the electrophysiological result (Fig. 6*I*,*J*). In contrast, glutamate evoked an increase in AIB Ca^{2+}i in *avr-14* animals ($t = 5.2$, df =

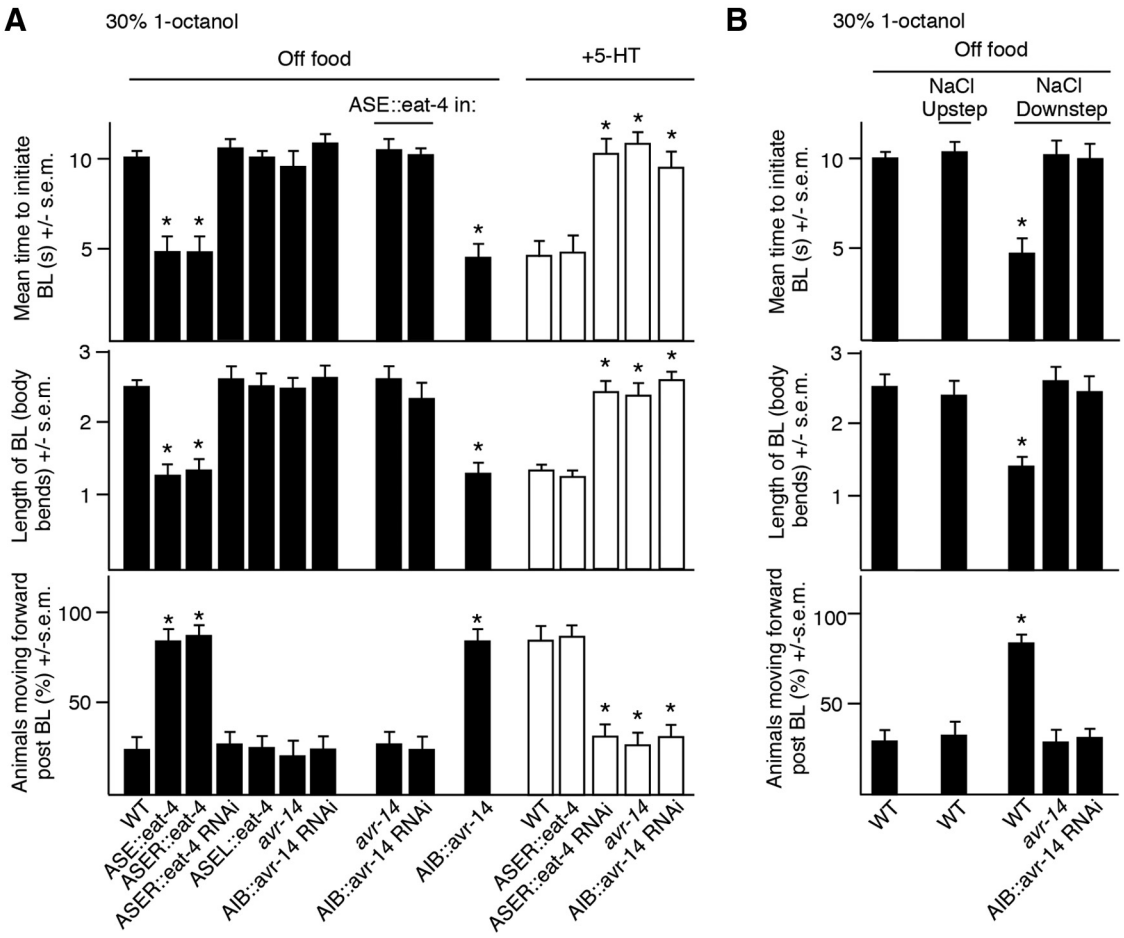

Figure 5. Activation of ASER modulates aversive responses. ***A***, Aversive responses to dilute 1-octanol without and with 4 mM 5-HT (black and white bars, respectively) were examined in wild-type and transgenic animals. *eat-4* was expressed in the ASEs, ASEL, and ASER using the *flp-6*, *gcy-6*, and *gcy-5* promoters, respectively. *eat-4* RNAi was expressed in ASER using the *gcy-5* promoter. *avr-14* and *avr-14* RNAi was expressed in the AIBs using the *inx-1* promoter. ***B***, Salt down-steps were performed by incubating animals for 10 min on a high-salt plate (+10 mM) and then transferring back to a NGM plate to be assayed. Salt up-steps were performed by incubating on an NGM plate and transferring to a high-salt plate (+10 mM) for 10 min before assaying. Data represent mean ± SEM with 15–20 animals being tested in 3 independent experiments and were analyzed by two-tailed Student's *t* test with Welch's correction. *$p < 0.001$, significantly different from wild-type animals under identical conditions.

57, $p < 0.001$; Fig. 6*I*,*J*), which was dependent on *glr-1* (i.e., glutamate-evoked Ca^{2+}i increases were absent in *avr-14;glr-1* animals; $t = 2.3$, df = 59, $p < 0.03$; Fig. 6*I*,*J*), confirming the excitatory role for GLR-1 in AIBs. Together, these results suggest that the AIBs express both excitatory and inhibitory glutamate receptors encoded by *glr-1* and *avr-14*, respectively, that function antagonistically to modulate the activity state of the AIBs.

Differential sensory-mediated modulation of the AIBs sharpens aversive responses

Dose–response curves to 1-octanol exhibit a plateau between 20% and 35% 1-octanol, followed by a shift from 10 to 5 s at concentrations >35% (Fig. 7*A*). In contrast, three different treatments predicted to inhibit AIB signaling, the inhibition of AWC signaling by the addition of IAA, the activation of ASER with a salt down-step, or the activation of HisCl1 in the AIBs, eliminated the plateau in the dose–response curve, with a shift to a more rapid initiation of the aversive response at much lower concentrations of repellant (Fig. 7*A*). In addition, this inhibition of AIB signaling also induced animals to move forward after the initial BL was complete regardless of the 1-octanol concentration; that is, if AIB signaling is inhibited, animals will ultimately continue toward the noxious odorant regardless of intensity the noxious stimulation (Fig. 7*B*) (Harris et al., 2011). Together, these data highlight a role for the AIBs in the integration of complex, often antagonistic sensory input and the potentially bimodal nature of AIB signaling in the modulation of aversive behavior and suggest that the inhibition of AIB signaling sensitizes aversive responses to lower repellant concentrations.

Discussion

Sensory inputs are extensively processed and integrated before decision making, with altered multisensory integration associated with disorders such as autism, depression, and schizophrenia (Iarocci and McDonald, 2006; Javitt, 2009; Farb et al., 2012). Sensorimotor control has been studied extensively in *C. elegans*, but, even in an organism with a relatively simple nervous system, much remains to be learned about how multiple sensory inputs are integrated to modulate locomotory behavior. In the present study, we have demonstrated that the two AIB interneurons integrate both tonic and acute antagonistic glutamatergic sensory inputs to modulate individual components of both spontaneous and repellant-dependent reversal differentially (Fig. 8).

During the approach to a noxious stimulus, 14 pairs of *C. elegans* sensory neurons continuously sample numerous intrinsic and extrinsic variables before determining a course of action,

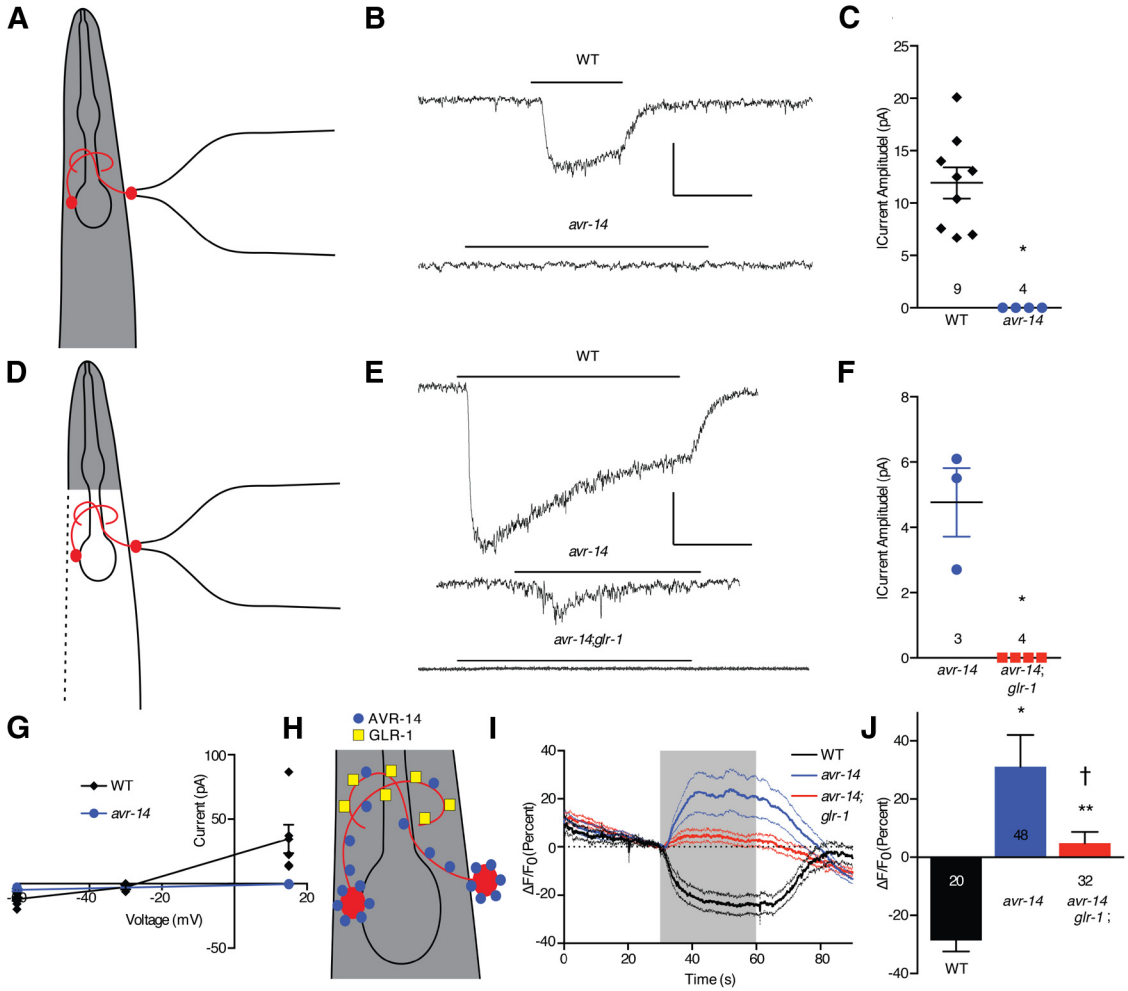

Figure 6. Glutamate responses in AIB neurons. ***A***, Diagram of partially dissected electrophysiology preparation. ***B***, Representative traces of glutamate-evoked currents in AIBs of wild-type and *avr-14* animals obtained using the partially dissected electrophysiology preparation (***A***). Vertical scale bar, 10 pA; horizontal scale bar, 1 s. ***C***, Quantitative comparison of glutamate-evoked currents obtained using the partially dissected electrophysiology preparation (***A***). Data are presented as mean ± SEM and were analyzed by two-tailed Student's *t* test with Welch's correction ($t = 8$, df = 8). *$p < 0.001$, significantly different from wild-type animals under identical conditions. Numbers above genotype indicate *n*. ***D***, Diagram of fully dissected electrophysiology preparation. ***E***, Representative traces of glutamate-evoked currents in AIBs of wild-type, *avr-14*, and *avr-14;glr-1* animals obtained using the fully dissected electrophysiology preparation (***D***). Vertical scale bar, 10 pA; horizontal scale bar, 1 s. ***F***, Quantitative comparison of glutamate-evoked currents obtained using the fully dissected electrophysiology preparation (***D***). Data are presented as mean ± SEM and were analyzed by two-tailed Student's *t* test with Welch's correction ($t = 4.5$, df = 2). *$p < 0.05$, significantly different from wild-type animals under identical conditions. Numbers above genotype indicate *n*. ***G***, Reversal potentials for glutamate-evoked currents in AIBs of nine wild-type (partially dissected) and three *avr-14* (fully dissected) animals. ***H***, Diagram depicting localization of AVR-14 on AIB cell bodies and neurites and localization of GLR-1 on AIB neurites. ***I***, Trace average of glutamate-evoked Ca^{2+}i transients in AIBs of wild-type, *avr-14*, and *avr-14;glr-1* animals obtained using fully dissected animals. ***J***, Comparison of maximum glutamate-evoked changes shown in ***H***. Data are presented as mean ± SEM and were analyzed by two-tailed Student's *t* test with Welch's correction ($t = 5.2$, df = 57, *$p < 0.001$ and $t = 6.1$, df = 49, **$p < 0.001$, significantly different from wild-type animals under identical conditions; $t = 2.3$, df = 60, †$p < 0.03$, significantly different from *avr-14* animals under identical conditions). Numbers within/beneath bars indicate *n*.

with the presence of food signaled by either distinct sensory neurons and/or endogenous serotonergic signaling inhibiting AIB signaling and encouraging animals to continue moving forward even in face of the noxious odor. Specifically, on food, 5-HT is released from the two NSMs, 5-HT levels are elevated, AIB signaling is inhibited through the 5-HT-gated Cl^- channel MOD-1, and, although animals initiate an aversive response more rapidly, they continue forward toward the noxious stimulus after the initial BL is complete (Harris et al., 2009; Harris et al., 2011). In contrast, off food, although animals initiate an aversive response more slowly, most animals execute an ω turn and move away from the noxious stimulus. Repellant dose–response curves in wild-type animals exhibit a plateau between 20% and 35% 1-octanol, with animals always moving away from the source of the repellant after the aversive response is initiated. In contrast, AIB inhibition removes the plateau from the dose–response curve, dramatically lowering the repellant concentration that initiates a more rapid aversive response, but paradoxically ensuring forward movement after the initial BL is complete regardless of the intensity of the repellant. Previous studies have always contended that food or 5-HT stimulate the aversive response based on more rapid initiation, but, in truth, food or 5-HT induce forward movement after the more rapid initiation of BL and limit the overall aversive response. That is, on 5-HT, the animals sense and respond more rapidly to the repellant, but ultimately choose to ignore it.

The *C. elegans* pharynx cannot pump efficiently when animals are moving backward and the modulatory system described in the present study ensures that, in the presence of food or select sensory outputs, the AIBs are inhibited and animals will continue to move toward food and feed even in the face of a noxious, potentially dangerous repellant (Raizen et al., 1995; Keane and

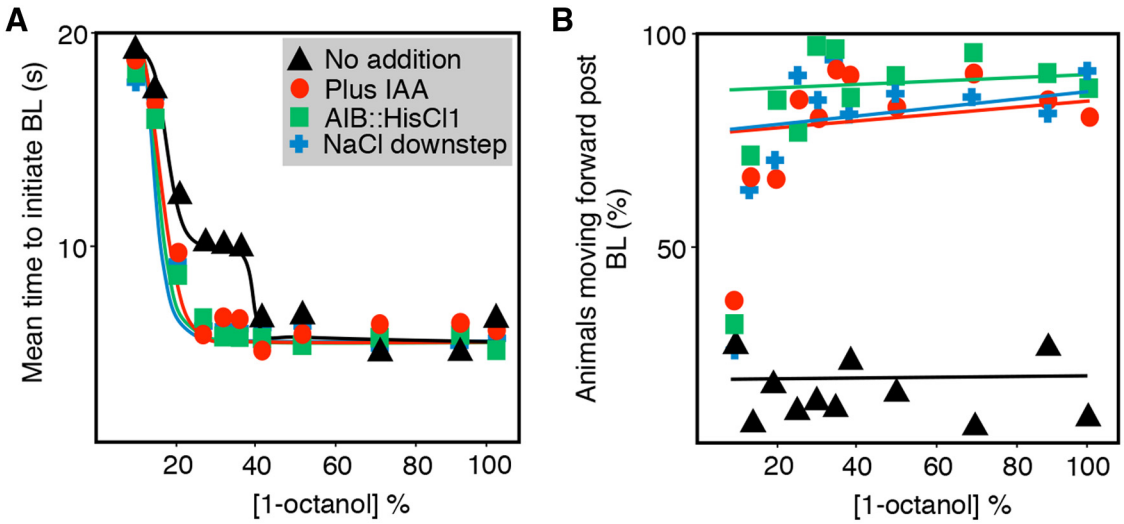

Figure 7. The two AIB interneurons integrate an array of sensory outputs to modulate both spontaneous and sensory-evoked reversals. ***A***, ***B***, Aversive responses to varying concentrations of 1-octanol were assayed in the presence and absence of 4 mM 5-HT and 40% IAA or after a salt down-step in wild-type animals. HisCl1 was expressed under the AIB-selective promoter *inx-1*. Data represent mean with 15–20 animals being tested in 3 independent experiments.

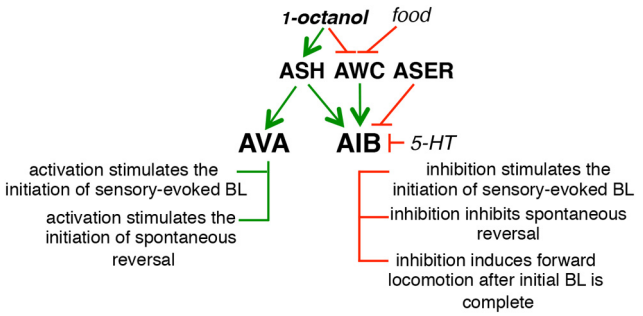

Figure 8. The AIBs integrate an array of sensory outputs and nutritional status to fine-tune aversive responses. Green arrows indicate stimulation and red arrows inhibition.

Avery, 2003). From an evolutionary perspective, animals that remain on food under these adverse conditions may have a selective advantage and decreasing the time that they are exposed to the aversive stimulus (i.e., decreasing the time taken to initiate BL) may shorten signaling to prevent the initiation of an ω turn. For example, the prolonged ASH and AIB signaling off food could trigger the release of additional modulatory neuropeptides or enhance signaling to the RIMs, the major synaptic partner of the AIBs that are involved in the initiation of an ω turn (Donnelly et al., 2013). Interestingly, a related flip/flop circuit modulating pharyngeal pumping has also been identified recently in *C. elegans*, in which pharyngeal pumping stimulated by the AWA sensory neurons remains constant in the face of an increasing concentration of repellant perceived by the ASHs until a critical repellant threshold is achieved, at which point pumping decreases rapidly (Li et al., 2012). Presumably, this system also facilitates maximal feeding in an unfavorable environment until the cost of the feeding becomes too great, at which point the animals cease feeding and presumably exit, suggesting that additional locomotory phenotypes also may couple to this flip/flop circuit associated with feeding, some of which are suggested by the present study.

In *C. elegans*, both spontaneous and sensory-evoked reversal is controlled by two distinct circuits, one involving the activation of the AVA backward command interneurons that synapse directly on the motor neurons and a second involving the disinhibition of a circuit favoring forward locomotion initiated by the two AIBs (Fig. 8; Gray et al., 2005; Piggott et al., 2011). The two interacting circuits may provide increased modulatory flexibility in the integration of multiple sensory inputs. Indeed, a similar dual system of motor initiation has been identified in mammals (Nambu, 2004). The two ASHs are the primary 1-octanol sensors, because ASH somal Ca^{2+}i increases in responses to 1-octanol and ASH ablation or the RNAi knock-down of ASH glutamatergic signaling abolishes the aversive response (Chao et al., 2004; Harris et al., 2010). The ASHs synapse directly on the AVAs and AIBs through the AMPA-like glutamate receptor GLR-1 to activate both arms of the reversal circuit (Mellem et al., 2002; Guo et al., 2009). For example, ASH activation, either by nose touch or increased osmolarity, is accompanied by *eat-4*- and *glr-1*-dependent increases in both AVA and AIB Ca^{2+}i and depolarization and the optogenetic activation of either the AVAs or AIBs in freely moving animals stimulates reversal, although whether this optogenetic activation mimics a physiological response is unclear because the optogenetic activation of the AIBs also has the potential to activate the AVAs directly though a gap junction network (Piggott et al., 2011). Most studies of AIB activation have focused on somal Ca^{2+}i signals, but the relationship between increased somal Ca^{2+}i and depolarization/ neurotransmitter release may not be as straightforward as previously assumed and recent work suggests that odorant-dependent changes in somal Ca^{2+}i may not reflect depolarization or neurotransmitter release in either the ASHs or ASEs faithfully (Oda et al., 2011; Luo et al., 2014; Zaharatka et al., 2015). Indeed, the somal Ca^{2+}i signal may be modulated extensively by downstream feedback and it has been suggested that Ca^{2+}i dynamics in the AIBs may not reflect sensory input, but rather motor feedback during navigation through complex sensory landscapes (Oda et al., 2011; Luo et al., 2014). It is interesting that increases in AIB Ca^{2+}i during nose touch occur well after the initiation of the sensory-evoked reversal (Piggott et al., 2011). Signaling from the AIBs to the RIMs, their major synaptic partner, is also complex, with both nose touch and osmolarity increasing ASH and AIB somal Ca^{2+}i, but nose touch decreasing and osmolarity increasing the Ca^{2+}i signal in the RIMs (Piggott et al., 2011). Similarly, the hyperpolarization of the

AIBs by the expression of HisCl1 decreases the length of BL and ω turns in response to osmolarity, but has no effect on the same parameters in response to nose touch (anterior touch/touch avoidance) (Pokala et al., 2014).

In addition to the ASHs, signaling from additional sensory neurons also appears to be integrated by the AIBs to modulate locomotory behavior (Fig. 8). For example, AWC somal Ca^{2+}i decreases in response to 1-octanol and, in contrast to ASH signaling, would be predicted to decrease AIB GLR-1 activation and AIB signaling, suggesting that the ASHs and AWCs may function antagonistically to fine-tune the aversive response. Similarly, signaling from ASER that responds to a host of additional environmental variables, but not 1-octanol, also appears to inhibit AIB signaling. For example, activation of ASER by ASER *eat-4* overexpression or a salt down-step causes a more rapid initiation of the aversive response and continued forward movement after BL, with both phenotypes requiring the expression the glutamate-gated Cl^- channel AVR-14 in the AIBs. Indeed, AIB:::AVR-14 overexpression in wild-type animals yields identical phenotypes. Importantly, additional sensory neurons, many of which also innervate the AIBs, appear to play are role in responses to ASH-aversive stimuli. For example, the FLPs are involved in nose touch and the ADLs and AWBs in response to 1-octanol (Hart et al., 1995; Chao et al., 2004). Together, these studies highlight the complex and highly modulated role of the AIBs in integrating an array of both acute and tonic outputs from multiple sensory neurons, with sensory inputs into the AIBs mediated by both excitatory and inhibitory glutamatergic signaling. A similar pattern of antagonistic glutamatergic signaling has been reported for the AIA interneurons (Chalasani et al., 2010).

The processing of multiple sensory modalities is essential for understanding our surroundings and initiating appropriate behaviors, with altered sensory processing associated with a host of conditions such as autism spectrum disorders (Brandwein et al., 2015; Zhang et al., 2014). Although most sensors are located peripherally, the problem appears to lie centrally in the integration of the sensory inputs, with these individuals incapable of perceiving auditory, visual, and tactile stimuli effectively (Ben-Sasson et al., 2009; Marco et al., 2011). The present study demonstrates that in *C. elegans* multiple sensory inputs are integrated by the two AIB interneurons and describes an excellent model system with which to understand how subtle sensory-dependent changes in AIB signaling can lead to markedly different behavioral outcomes. Future studies will focus on how these different sensory inputs modulate AIB signaling to its downstream synaptic partners.

References

Arena JP, Liu KK, Paress PS, Schaeffer JM, Cully DF (1992) Expression of a glutamate-activated chloride current in *Xenopus* oocytes injected with *Caenorhabditis elegans* RNA: evidence for modulation by avermectin. Brain Res Mol Brain Res 15:339–348. CrossRef Medline

Ben-Sasson A, Hen L, Fluss R, Cermak SA, Engel-Yeger B, Gal E (2009) A meta-analysis of sensory modulation symptoms in individuals with autism spectrum disorders. J Autism Dev Disord 39:1–11. CrossRef Medline

Brandwein AB, Foxe JJ, Butler JS, Frey HP, Bates JC, Shulman LH, Molholm S (2015) Neurophysiological indices of atypical auditory processing and multisensory integration are associated with symptom severity in autism. J Autism Dev Disord 45:230–244. Medline

Busch KE, Laurent P, Soltesz Z, Murphy RJ, Faivre O, Hedwig B, Thomas M, Smith HL, de Bono M (2012) Tonic signaling from O(2) sensors sets neural circuit activity and behavioral state. Nat Neurosci 15:581–591. CrossRef Medline

Chalasani SH, Chronis N, Tsunozaki M, Gray JM, Ramot D, Goodman MB, Bargmann CI (2007) Dissecting a circuit for olfactory behaviour in *Caenorhabditis elegans*. Nature 450:63–70. CrossRef Medline

Chalasani SH, Kato S, Albrecht DR, Nakagawa T, Abbott LF, Bargmann CI (2010) Neuropeptide feedback modifies odor-evoked dynamics in *Caenorhabditis elegans* olfactory neurons. Nat Neurosci 13:615–621. CrossRef Medline

Chao MY, Komatsu H, Fukuto HS, Dionne HM, Hart AC (2004) Feeding status and serotonin rapidly and reversibly modulate a *Caenorhabditis elegans* chemosensory circuit. Proc Natl Acad Sci U S A 101:15512–15517. CrossRef Medline

Conradt B, Horvitz HR (1998) The *C. elegans* protein EGL-1 is required for programmed cell death and interacts with the Bcl-2-like protein CED-9. Cell 93:519–529. CrossRef Medline

Cook A, Aptel N, Portillo V, Siney E, Sihota R, Holden-Dye L, Wolstenholme A (2006) *Caenorhabditis elegans* ivermectin receptors regulate locomotor behaviour and are functional orthologues of *Haemonchus contortus* receptors. Mol Biochem Parasitol 147:118–125. CrossRef Medline

Dent JA, Smith MM, Vassilatis DK, Avery L (2000) The genetics of ivermectin resistance in *Caenorhabditis elegans*. Proc Natl Acad Sci U S A 97:2674–2679. CrossRef Medline

Donnelly JL, Clark CM, Leifer AM, Pirri JK, Haburcak M, Francis MM, Samuel AD, Alkema MJ (2013) Monoaminergic orchestration of motor programs in a complex *C. elegans* behavior. PLoS Biol 11:e1001529. CrossRef Medline

Esposito G, Di Schiavi E, Bergamasco C, Bazzicalupo P (2007) Efficient and cell specific knock-down of gene function in targeted *C. elegans* neurons. Gene 395:170–176. CrossRef Medline

Farb NA, Anderson AK, Segal ZV (2012) The mindful brain and emotion regulation in mood disorders. Can J Psychiatry 57:70–77. Medline

Francis MM, Maricq AV (2006) Electrophysiological analysis of neuronal and muscle function in *C. elegans*. Methods Mol Biol 351:175–192. CrossRef Medline

Ghanizadeh A (2011) Sensory processing problems in children with ADHD, a systematic review. Psychiatry Investig 8:89–94. CrossRef Medline

Goodman MB, Hall DH, Avery L, Lockery SR (1998) Active currents regulate sensitivity and dynamic range in *C. elegans* neurons. Neuron 20:763–772. CrossRef Medline

Gray JM, Hill JJ, Bargmann CI (2005) A circuit for navigation in *Caenorhabditis elegans*. Proc Natl Acad Sci U S A 102:3184–3191. CrossRef Medline

Guo ZV, Hart AC, Ramanathan S (2009) Optical interrogation of neural circuits in *Caenorhabditis elegans*. Nat Methods 6:891–896. CrossRef Medline

Haider B, Duque A, Hasenstaub AR, McCormick DA (2006) Neocortical network activity in vivo is generated through a dynamic balance of excitation and inhibition. J Neurosci 26:4535–4545. CrossRef Medline

Hanson JL, Hurley LM (2014) Context-dependent fluctuation of serotonin in the auditory midbrain: the influence of sex, reproductive state and experience. J Exp Biol 217:526–535. CrossRef Medline

Hapiak V, Summers P, Ortega A, Law WJ, Stein A, Komuniecki R (2013) Neuropeptides amplify and focus the monoaminergic inhibition of nociception in *Caenorhabditis elegans*. J Neurosci 33:14107–14116. CrossRef Medline

Harris GP, Hapiak VM, Wragg RT, Miller SB, Hughes LJ, Hobson RJ, Steven R, Bamber B, Komuniecki RW (2009) Three distinct amine receptors operating at different levels within the locomotory circuit are each essential for the serotonergic modulation of chemosensation in *Caenorhabditis elegans*. J Neurosci 29:1446–1456. CrossRef Medline

Harris G, Mills H, Wragg R, Hapiak V, Castelletto M, Korchnak A, Komuniecki RW (2010) The monoaminergic modulation of sensory-mediated aversive responses in *Caenorhabditis elegans* requires glutamatergic/peptidergic cotransmission. J Neurosci 30:7889–7899. CrossRef Medline

Harris G, Korchnak A, Summers P, Hapiak V, Law WJ, Stein AM, Komuniecki P, Komuniecki R (2011) Dissecting the serotonergic food signal stimulating sensory-mediated aversive behavior in *C. elegans*. PLoS One 6:e21897. CrossRef Medline

Hart AC, Sims S, Kaplan JM (1995) Synaptic code for sensory modalities revealed by *C. elegans* GLR-1 glutamate receptor. Nature 378:82–85. CrossRef Medline

Hobert O (2002) PCR fusion-based approach to create reporter gene constructs for expression analysis in transgenic *C. elegans*. Biotechniques 32:728–730. Medline

Iarocci G, McDonald J (2006) Sensory integration and the perceptual expe-

rience of persons with autism. J Autism Dev Disord 36:77–90. CrossRef Medline

Javitt DC (2009) Sensory processing in schizophrenia: neither simple nor intact. Schizophr Bull 35:1059–1064. CrossRef Medline

Kantrowitz JT, Javitt DC (2010) Thinking glutamatergically: changing concepts of schizophrenia based upon changing neurochemical models. Clin Schizophr Relat Psychoses 4:189–200. CrossRef Medline

Keane J, Avery L (2003) Mechanosensory inputs influence *Caenorhabditis elegans* pharyngeal activity via ivermectin sensitivity genes. Genetics 164: 153–162. Medline

Kohn RE, Duerr JS, McManus JR, Duke A, Rakow TL, Maruyama H, Moulder G, Maruyama IN, Barstead RJ, Rand JB (2000) Expression of multiple UNC-13 proteins in the *Caenorhabditis elegans* nervous system. Mol Biol Cell 11:3441–3452. CrossRef Medline

Kramer JM, French RP, Park EC, Johnson JJ (1990) The *Caenorhabditis elegans* rol-6 gene, which interacts with the sqt-1 collagen gene to determine organismal morphology, encodes a collagen. Mol Cell Biol 10:2081–2089. Medline

Leinwand SG, Chalasani SH (2013) Neuropeptide signaling remodels chemosensory circuit composition in *Caenorhabditis elegans*. Nat Neurosci 16:1461–1467. CrossRef Medline

Li Z, Li Y, Yi Y, Huang W, Yang S, Niu W, Zhang L, Xu Z, Qu A, Wu Z, Xu T (2012) Dissecting a central flip-flop circuit that integrates contradictory sensory cues in *C. elegans* feeding regulation. Nat Commun 3:776. CrossRef Medline

Lindsay TH, Thiele TR, Lockery SR (2011) Optogenetic analysis of synaptic transmission in the central nervous system of the nematode *Caenorhabditis elegans*. Nat Commun 2:306. CrossRef Medline

Luo L, Wen Q, Ren J, Hendricks M, Gershow M, Qin Y, Greenwood J, Soucy ER, Klein M, Smith-Parker HK, Calvo AC, Colón-Ramos DA, Samuel AD, Zhang Y (2014) Dynamic encoding of perception, memory, and movement in a *C. elegans* chemotaxis circuit. Neuron 82:1115–1128. CrossRef Medline

Marco EJ, Hinkley LB, Hill SS, Nagarajan SS (2011) Sensory processing in autism: a review of neurophysiologic findings. Pediatr Res 69:48R–54R. CrossRef Medline

Mellem JE, Brockie PJ, Zheng Y, Madsen DM, Maricq AV (2002) Decoding of polymodal sensory stimuli by postsynaptic glutamate receptors in *C. elegans*. Neuron 36:933–944. CrossRef Medline

Mello CC, Kramer JM, Stinchcomb D, Ambros V (1991) Efficient gene transfer in C.elegans: extrachromosomal maintenance and integration of transforming sequences. EMBO J 10:3959–3970. Medline

Mills H, Hapiak V, Harris G, Summers P, Komuniecki R (2012a) The interaction of octopamine and neuropeptides to slow aversive responses in *C. elegans* mimics the modulation of chronic pain in mammals. Worm 1:202–206. CrossRef Medline

Mills H, Wragg R, Hapiak V, Castelletto M, Zahratka J, Harris G, Summers P, Korchnak A, Law W, Bamber B, Komuniecki R (2012b) Monoamines and neuropeptides interact to inhibit aversive behaviour in *Caenorhabditis elegans*. EMBO J 31:667–678. CrossRef Medline

Mueller-Pfeiffer C, Schick M, Schulte-Vels T, O'Gorman R, Michels L, Martin-Soelch C, Blair JR, Rufer M, Schnyder U, Zeffiro T, Hasler G (2013) Atypical visual processing in posttraumatic stress disorder. Neuroimage Clin 3:531–538. CrossRef Medline

Nambu A (2004) A new dynamic model of the cortico-basal ganglia loop. Prog Brain Res 143:461–466. Medline

Oda S, Tomioka M, Iino Y (2011) Neuronal plasticity regulated by the insulin-like signaling pathway underlies salt chemotaxis learning in *Caenorhabditis elegans*. J Neurophysiol 106:301–308. CrossRef Medline

Piggott BJ, Liu J, Feng Z, Wescott SA, Xu XZ (2011) The neural circuits and synaptic mechanisms underlying motor initiation in *C. elegans*. Cell 147: 922–933. CrossRef Medline

Pokala N, Liu Q, Gordus A, Bargmann CI (2014) Inducible and titratable silencing of *Caenorhabditis elegans* neurons in vivo with histamine-gated chloride channels. Proc Natl Acad Sci U S A 111:2770–2775. CrossRef Medline

Raizen DM, Lee RY, Avery L (1995) Interacting genes required for pharyngeal excitation by motor neuron MC in *Caenorhabditis elegans*. Genetics 141:1365–1382. Medline

Speese S, Petrie M, Schuske K, Ailion M, Ann K, Iwasaki K, Jorgensen EM, Martin TF (2007) UNC-31 (CAPS) is required for dense-core vesicle but not synaptic vesicle exocytosis in *Caenorhabditis elegans*. J Neurosci 27: 6150–6162. CrossRef Medline

Suzuki H, Thiele TR, Faumont S, Ezcurra M, Lockery SR, Schafer WR (2008) Functional asymmetry in *Caenorhabditis elegans* taste neurons and its computational role in chemotaxis. Nature 454:114–117. CrossRef Medline

White JG, Southgate E, Thomson JN, Brenner S (1986) The structure of the nervous system of the nematode *Caenorhabditis elegans*. Philos Trans R Soc Lond B Biol Sci 314:1–340. CrossRef Medline

Wragg RT, Hapiak V, Miller SB, Harris GP, Gray J, Komuniecki PR, Komuniecki RW (2007) Tyramine and octopamine independently inhibit serotonin-stimulated aversive behaviors in *Caenorhabditis elegans* through two novel amine receptors. J Neurosci 27:13402–13412. CrossRef Medline

Zahratka JA, Williams PD, Summers PJ, Komuniecki RW, Bamber BA (2015) Serotonin differentially modulates Ca++ transients and depolarization in a *C. elegans* nociceptor. J Neurophysiol 113:1041–1050. Medline

Zhang Y, Bonnan A, Bony G, Ferezou I, Pietropaolo S, Ginger M, Sans N, Rossier J, Oostra B, LeMasson G, Frick A (2014) Dendritic channelopathies contribute to neocortical and sensory hyperexcitability in Fmr1 mice. Nat Neurosci 17:1701–1709. CrossRef Medline